IOP Conf. Series: Journal of Physics: Conf. Series **823** (2017) 012008 doi:10.1088/1742-6596/823/1/012008

Radio frequency emissions from laser induced material breakdown

Vinoth Kumar[1], Manikanta Elle[1] and Prem Kiran Paturi[1]

[1]Advanced centre of research in high energy materials (ACRHEM), University of Hyderabad, Gachibowli, Hyderabad 500 046, India

E-mail: premkiranuoh@gmail.com

Abstract. Observation of radio frequency (RF) emissions from laser induced breakdown (LIB) of stainless steel (SS304) and the studies on the origin of these emissions are presented. The emitted frequencies were observed to be in the range of the estimated ion-plasma frequencies, indicating the contribution of the ion-neutral collisional interactions in the radiation of RF emissions from plasma. These studies can be extended to develop an RF based tool to study the plasmas of varying electron temperatures and densities.

1. Introduction

The low frequency emissions from plasma and their applications have been widely investigated for several decades [1]. The RF and microwave radiations generated from plasmas due to laser induced breakdown (LIB) [2,3] have been studied to make them feasible for applications like laser ground penetrating radars (LGPR) [4] that has several advantages when compared with the conventional GPR. From our studies, the spectral selective RF emissions from nanosecond (ns) and picosecond (ps) LIB of different targets, that can be developed into a sample identification tool, was understood [5]. These emissions were mainly observed due to the ion plasma frequencies due to the atomic and molecular ionized species [6]. By varying the input laser parameters, plasmas with varying electron temperatures and densities hence varying plasma ion frequencies can be created, making the study of RF emissions a generic tool for plasma diagnostics. For example, in tokomak plasmas [7], the α particles, emitted during the fusion process, due to their cyclotronic gyration in the confining magnetic field are predicted to give rise to radio frequency (RF) emissions in 10-500 MHz band [8]. Experimental observation of RF emissions due to fast ions situated in the core of the discharge were reported to be useful in extracting the information concerning the fusion products [9]. Though the plasma is actively held away from the walls of the tokamak container by using powerful magnetic fields, sometimes the plasma can interact with the inner walls of the reactor which might result in plasma contamination. Therefore, understanding the RF emissions from tokamak plasmas pave way to study the thermal contaminants present in the plasma system over long duration. In this paper, we report the observation and the origin of RF emissions from the LIB of stainless steel (SS304), which is one of the important materials considered for the tokamak walls.

2. Experiment

Second harmonic (532 nm) of Nd:YAG lasers of different pulse durations (7 ns and 30 ps) were focused, in the focal geometry (f/D) ~ 10 and 6.5 in the ns and ps regimes respectively, on the target (SS304) to generate LIB. The laser intensities in case of ns LIB and ps LIB are of the orders of ~10^{11}

W/cm^2 and ~10^{13} W/cm^2 respectively. The RF emission detection was carried out with a broadband mini biconical antenna (Lindgren 3182) of frequency range 30 MHz – 1 GHz while the waveforms were recorded with a spectrum analyzer (Agilent PSA E4448A) which can scan over 3 Hz – 50 GHz, giving rise to the frequency evolution over the entire band of the detecting antenna at a single shot. The polarization state of ns and ps laser pulses was vertical and horizontal, respectively. As depicted in figure 1(a), the antenna polarization is termed as vertical (V-pol), whenever it is oriented parallel to the x-axis. When it is rotated parallel to the y-axis, it is termed as horizontal antenna polarization (H-pol). The antenna was rotated to measure the H-pol and V-pol components of emissions. Single shot-LIB was ensured with the target mounted on an electronically controlled XY translation stages (M-443, LTA-HA, and ESP-300, M/s. Newport). In order to cut down the contribution of ambient RF noises, the spectra without plasma formation (noise) was subtracted from the LIB data that contains noise and the signals of interest. Besides, the average RF spectrum from the LIB of atleast 100 laser shots was considered for data analysis. The spectrum analyzer was externally triggered by the laser pulse to ensure better signal to noise ratio of the recorded spectra [10].

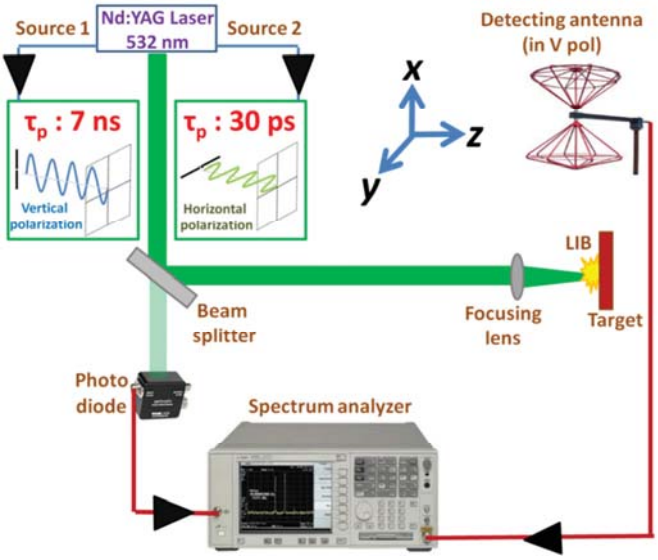

Figure 1. (a) Experimental setup with laser propagating along z direction.

Before proceeding with the experiments, it is important to position the detector at the point where maximum radiation is received. Therefore, the angular distribution of RF emissions from the LIB of a solid target (copper) was studied by detecting the RF emissions from LIB at different angles between the source and the detector, by keeping the distance fixed. The amplitude of RF emissions from ns LIB and ps LIB were observed to be increasing with the angle between the source and the detector with the maximum when the source and the detector are perpendicular to each other (90º and 270º). In order to arrive at the integrated power of RF emissions from LIB of the targets, the frequency domain RF spectra were converted into the corresponding time domain spectra by inverse fast Fourier transformation (IFFT). The area under the curve of the time domain spectrum gives the total energy output of the emitted RF radiation. The total output energy is normalized with respect the solid angle subtended by the detector. This is termed as the normalized RF output. The fit of normalized RF with respect to of angle of detection is given in figure 2.

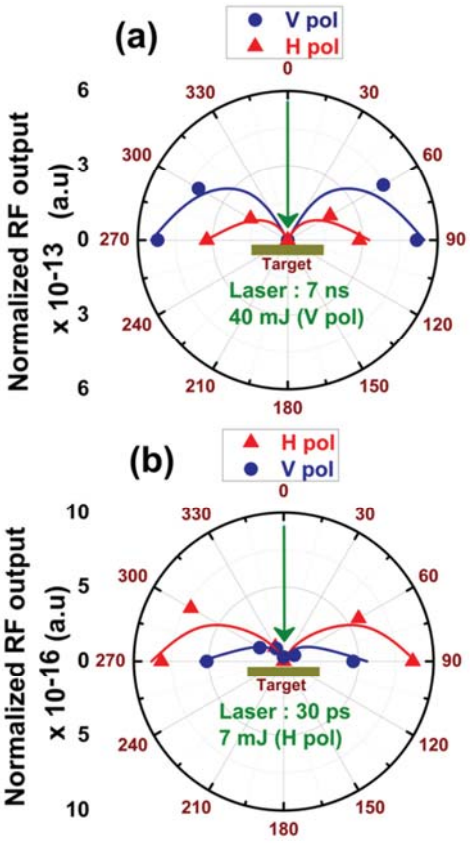

Figure 2. (a) Angular distribution of RF emissions from (a) 7 ns LIB at 40 mJ and (b) 30 ps LIB at 7 mJ of solid target (copper) under different antenna polarization.

The best fits for the angular distribution of normalized RF emissions were turned out to vary as $\sin^{1.6}\theta$ and $\sin^{1.5}\theta$ in case of ns and ps LIB, respectively, for the laser and antenna polarizations used in the present study. Hence, the $\sin^2\theta$ dependence of RF emissions was confirmed in case of solid targets. The dipolar emission pattern ($\sin^2\theta/r^2$) [11] was confirmed from the RF emissions from LIB of atmospheric air [6]. Thus, in our studies, antenna was positioned, closer to the plasma source (~ 1 metre), perpendicular to the laser propagation direction. It is also observed that the emissions with same laser and antenna polarization were observed to be stronger than those with cross polarization. Therefore, the analyses were emphasized with same laser and antenna polarization conditions.

3. Results and discussion

The RF emissions from ns and ps LIB of SS304, at different input laser energies, are given in Figure 3. The emissions were observed to be strongly dependent on the laser parameters (pulse duration, input laser energy etc.). The dominant RF emissions from ns and ps LIB were observed to be spread within 300 MHz barring few relatively less intense peaks at higher frequencies. From the positioning of the frequency peaks, it is confirmed that no harmonic signals are observed from the LIB. This shows that the frequency lines represent the RF emissions from the LIB of the target medium. Both in ns and ps LIB, the RF emissions at lower input laser energies were observed to be higher than those at higher input laser energies. When compared with the emissions from ns LIB, the emissions from ps LIB were observed to be 2-3 orders lesser.

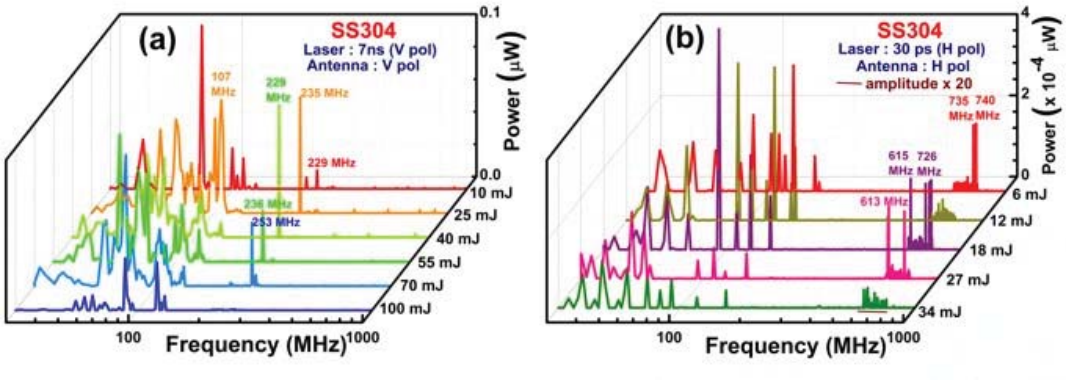

Figure 3. RF emissions from (a) 7 ns and (b) 30 ps LIB of SS304 under same laser and antenna polarization. *The line in 3 (b) represents the amplified portion of the spectrum for the better view of the frequencies*

The interaction of the plasma constituents, as depicted in figure 4, will result either in the growth (further ionization) or decay (recombination) of plasma and the corresponding energy release [12]. The RF emissions from LIB depend on the degree of ionization that determines the plasma number density (n_e, n_i) which in turn depends on the laser parameters (energy, pulse duration etc.) and the plasma recombination. In underdense plasmas as in our case, the interaction of charged particles with atomic clusters will be dominant [13]. These charge-neutral interactions give rise to emissions in the RF and microwave range of frequencies [1, 14] as shown in figure 4. Therefore, the RF emissions take place as long as there is interaction between the charged particles and the neutrals in the plasma system. Evidently, the RF emissions were observed to be relatively higher at lower input laser energies where the electron-neutral interaction remains higher (figure 3). As the ionization is higher with the ps pulses, due to relatively higher peak power when compared to the ns pulses, resulting in lower probability of charge-neutral interactions. Moreover, the rate of recombination is relatively higher in plasma due to ps LIB. Thus the emitted RF powers from ps LIB are lower than those from ns LIB. Besides the emissions due to charge-neutral interactions, RF emissions also take place owing to the oscillations of the dipoles that are formed due to the difference in the drift velocities of the electrons (~1500 m/s) and the ions (~5 m/s) [4]. However, after a certain value of input laser intensity, the damping of plasma brings down the emission of radiation. The damping of the plasma oscillations is predominantly due to collision/recombination and electron-attachment [13]. According to the recombination model, the loss of plasma by recombination is proportional to the product of electron and ion number densities ($n_e \times n_i$). At moderate input laser intensities, the number of charged species and their velocities in the underdense plasma is relatively lower and hence the charge particle-neutral collisions are dominant. In this case, the relaxation time for the kinetic energy of the electrons, which is proportional to the electron temperature, is longer than that for the average velocity (of the ions and neutrals) by a factor of (m_n/m_e) [12,13]. Therefore, the RF emissions were observed to be higher at moderate input intensities. At higher laser intensities, the higher value of n_e (n_i) and also the temperature of the electrons leads to the interaction between the plasma constituents. In this case, recombination will take place at a faster rate, when compared to that in plasmas due to lower input intensities, reducing the plasma density more drastically. Thus the RF emissions come down at higher input intensities. This is reflected in the data presented in figure 3.

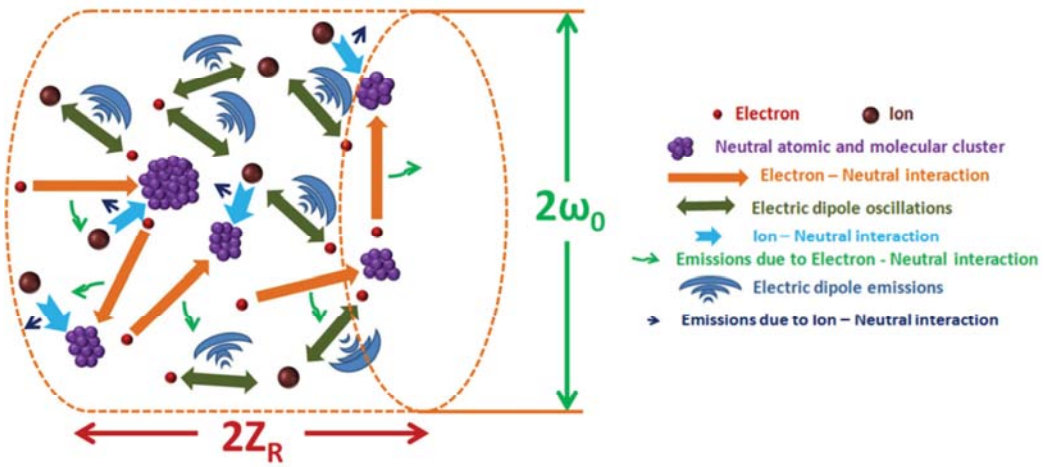

Figure 4. RF emission mechanisms from LIB of target material

Further, to arrive at the origin of these emissions, the ion plasma frequencies (ω_{pi}) were estimated using the following equation.

$$\omega_{pi}^2 = \frac{n_i Z^2 e^2}{m_i \varepsilon_0} \quad (1)$$

where n_i is the ion number density, Z and m_i are the charge state and mass of the ions respectively. In our case, the atoms are considered to be singly ionized. Therefore, Z is taken to be one and hence $n_e = n_i$. The target material (SS304) was studied to be composed of Fe (~ 72%), Cr (~ 18%), and Ni (~ 8%) and Mn (~1%). The value of $n_i = n_e$, under the studied range of laser intensities were obtained from literature [15]. The ω_{pi} values corresponding to the different possible atomic and molecular species in the LIB of SS304 were estimated and given in table 1.

Table 1. Estimated ion-plasma frequency (ω_{pi}) values

Laser	Intensity range (W/cm^2)	Electron density range (m^{-3})	Estimated ion-plasma frequency values (MHz)	
			Atomic species	Molecular species
7 ns	$3 - 7\times10^{10}$	$1 - 3\times10^{17}$	Fe^+: 235 Mn^+: 236 Cr^+: 243 Ni^+: 229	$(Fe_2O_3)^+$: 110 $(Mn_3O_4)^+$: 110
30 ps	$1 - 4\times10^{12}$	$7 - 10\times10^{18}$	Fe^+: 1247 Ni^+: 1216 Mn^+: 1257 Cr^+: 1292	$(Fe_3O_4)^+$: 612 $(Fe_2O_3)^+$: 737 $(Mn_3O_4)^+$: 616 $(Mn_2O_3)^+$: 742 $(Ni_2O_3)^+$: 725

It is evident that the emitted radio frequencies, shown in figures 3(a) and (b), correspond to the estimated ion-plasma frequencies shown in table 1. This shows the importance of the ionization and ion-neutral interactions in the RF emissions from the underdense plasma due to LIB. The estimated ω_{pi} values are observed with ± 3 MHz frequency error, which is the minimum frequency that the spectrum analyzer can resolve. The ω_{pi} values, corresponding to the atomic species, in ps LIB were observed to

be in GHz range which is beyond the detection range of the antenna. However, some of the peaks in the MHz region can be accounted for the contributions from the oxides (molecular species) of the elements present in the system. Owing to relatively smaller velocity of the charged particles (electrons and ions) that collide with the neutrals, the RF power of high frequency emissions (250-760 MHz) is relatively lower than that of the low frequency emissions (30-250 MHz). Moreover, in case of ps LIB, the charge-neutral interaction will be relatively low. This is reflected from the low amplitude of emissions in case of ps LIB. Therefore, the RF emissions from LIB can be useful in extracting the elemental information of the target.

4. Conclusion

The studies on RF emissions from LIB of SS304 were carried out. The emitted frequencies from LIB were observed to be in the range of estimated ion-plasma frequency ω_{pi}. Therefore, the emissions can be attributed to the contribution of ion-neutral interactions to the radiation emissions from the plasma source. These studies can be extended to develop an RF based tool to study the plasmas of varying electron temperatures and densities. By varying the input laser parameters (energy, polarization, pulse duration), plasmas with varying electron temperatures and densities hence varying plasma ion frequencies can be created, making the study of RF emissions a generic tool for plasma diagnostics.

Acknowledgement

The authors thank DRDO, Government of India, for the grants-in-aid support.

References

[1] Bekefi G 1966 *Radiation processes in plasmas* (Wiley)
[2] Pearlman J S and Dahlbacka G H 1978, *J. Appl. Phys.* **49**, 457
[3] Gerdin G and Tanist M J 1986, *Plasma Phys. Control.* Fusion **28**, 527
[4] Nakajima H, Shimada Y, Somekawa T, Fujita M and Tanaka K A 2009, *IEEE Geosci. Remote Sens. Lett.* **6**, 718
[5] Vinoth Kumar L, Manikanta E, Leela Ch and Prem Kiran P 2014, *Appl. Phys. Lett.* **105**, 064102
[6] Vinoth Kumar L, Manikanta E, Leela Ch and Prem Kiran P 2016, *J. Appl. Phys.* **119**, 214904
[7] McCracken G and Stott P 2005, *Fusion the energy of the universe* (Elsevier academic press)
[8] Kadomtsev B B 1992 *Tokamak plasma: A complex physical system* (Taylor & Francis group)
[9] Fraboulet D 1996 *Ion cyclotron emission in tokamak plasmas* (PhD dissertation, Grenoble Univ)
[10] Vinoth Kumar L, Leela Ch, Manikanta E, Tewari S P and Prem Kiran P 2012, *Proc SPIE.* **8434**, 84340V1
[11] Jackson J D 1998 *Classical Electrodynamics* (Wiley)
[12] Chen F F 1984 *Introduction to plasma physics and controlled fusion vol 1: plasma physics* (Plenum press)
[13] Bittencourt J A 2004 *Fundamentals of plasma physics*(Springer)
[14] Akcasu A Z and Wald L H 1967, *Phys. Fluids* **10**, 1327
[15] Singh J P and Thakur S N 2007 *Laser-Induced Breakdown Spectroscopy* (Elsevier Science)